

Design of Dual Frequency Coupled Resonators Using DGS and Microstrip Resonators for Dual Band WPT Applications

Hany A. Atallah¹, Musallam Alzubi², Rasha Hussein¹, and Adel B. Abdlerhman^{1,3}

¹Electrical Engineering Department, Faculty of Engineering, South Valley University, Qena 83523, Egypt
h.atallah@eng.svu.edu.eg, rasha.h.ahmed@eng.svu.edu.eg

²Ministry of Communications, Po Box 318, Safat 11111, Kuwait

³School of Electronics, Communications and Computer Engineering, Egypt-Japan University of Science and Technology, Alexandria 21934, Egypt

Abstract — This paper introduces a new design for a highly efficient and more compact size dual frequency wireless power transfer (WPT) system, which can operate at both 0.65 GHz and 1.56 GHz bands. The idea of the structure depends on designing a symmetrical system containing Tx and Rx. Each Tx and Rx has a feed line on the top layer with two stubs; each stub has different dimensions than the other one. The bottom layer contains two C-shaped defected ground structures (DGS). By changing the dimensions of one stub, the frequency resonance corresponds to this stub is changed without any change on the other resonance. The system has a size of 20×20 mm². Further, the system achieves efficiencies of 72 % and 89 % at 0.65 GHz and 1.56 GHz, respectively with a transmission distance of 8 mm. The proposed dual frequency WPT is implemented and verified. Good concurrences among electromagnetic (EM) simulations and the measurements have been attained. The system is suitable for recharging short-range applications.

Index Terms — Dual Band (DB), stub, Wireless Power Transfer (WPT).

I. INTRODUCTION

Wireless power transfer (WPT) technology comes with the promise of cutting the last cord by allowing recharge electronics devices as easily as data and the power will be transferred through the air without cables. WPT technology has been attracted many researchers in recent and previous periods for its impact in numerous prospective uses for instance sensor networks, controllable automated equipment (tablets, mobile phones, etc.), RFIDs, and so on [1-5]. The size of the system (particularly the receiver), the power transferring distance, and the efficiency are the furthestmost key factors to be addressed in designing the building blocks of the WPT systems. Initially, the researchers have

employed the coils for designing WPT systems and they have investigated the effects of the coil's parameters on the coupling efficiency and the working frequency. WPT is now applied as a viable method to power many types of devices including portable consumer electronics [6], electric vehicles [7], and biomedical implants [8]. Numerous of the short-range WPT methods are employing lumped components [9]. However, these components have sensible drawbacks in execution such as occupying an excessive space. In addition, they are lossy. Nonetheless, they are preferred in WPT applications at low frequencies.

Newly, defected ground structure (DGS) is the innovative technology that is presently used for designing WPT systems [10-13]. Some designs of the DGS are investigated and implemented for WPT like the C-shaped design [14]. Most of the published ideas investigate the usage of the modified DGS for obtaining single band operations [15].

Lately, they have improved the DGS to realize a dual band near-field WPT system [16-18]. However, the dual-band WPT has many benefits over the single band systems as implemented in [16]. The authors in [10] studied the WPT system by employing the DGS technique. Firstly, they suggested an H-shaped DGS with a size of 25×25 mm² and an efficiency of 68% at 0.3 GHz at a transmission distance of 5 mm. Secondly, the structure is enhanced and developed to be semi H-shaped. The system has a size of 20×20 mm² with an efficiency of 73%. In [11], a dual frequency system is proposed. Further, it depends on two circular DGS resonators whereas each circular is responsible for frequency resonance. The system has a size of 30×15 mm² and the efficiencies are 71% and 71% at 0.3 GHz and 0.7 GHz with a transmission distance of 16 mm. In [17], a dual band system is proposed with a size of 12.5×8.9 cm² and efficiencies of 78% and 70.6% at 6.78 MHz and 200 kHz, respectively. In [19], the author

introduced a dual-band rectifying circuit for wireless power transmission working at 2.45 GHz and 5.8 GHz. This system showed peak RF-to-DC efficiencies of 66.8% and 51.5% at 2.45 GHz and 5.8 GHz, respectively.

Recently, the DGS resonators are extensively explored for single and dual band operations of the WPT applications [10-12,15,18-22].

In this paper, a new dual frequency WPT system is proposed. The system introduces a new idea which designs two stubs with different sizes for obtaining dual band frequencies. The size of the system is $20 \times 20 \text{ mm}^2$ with efficiencies of 72% and 89% at 0.65 and 1.56 GHz, respectively.

II. COUPLED RESONATOR DESIGN

Listed below the configuration of the suggested dual frequency system. Figure 1 (a) shows the top view which contains a feed line with a width of W_f and a length of 19.5 mm. The stubs are designed on the top with different sizes, that responsible for dual band frequency operation. Figure 1 (b) shows the bottom layer which contains a C-shaped DGS with the same shorted points connected with the top view. The design parameters are recorded in Table 1. Figure 2 (a) shows the setting of the suggested geometry of the coupled resonators which are parted by a space of h mm. Figure 2 (b) represents the equivalent circuit of the system. The equivalent circuit presents a dual band resonance circuit and each circuit is considered as a separate one. The equivalent circuit contains $(L_{p1}$ and $C_{p1})$ which are the parallel elements of the tank circuit related to the first resonance frequency and $(L_{p3}$ and $C_{p3})$ are related to the second resonance frequency.

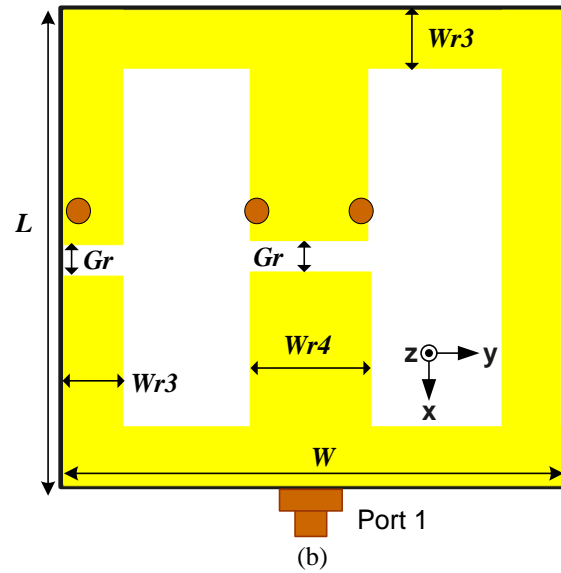
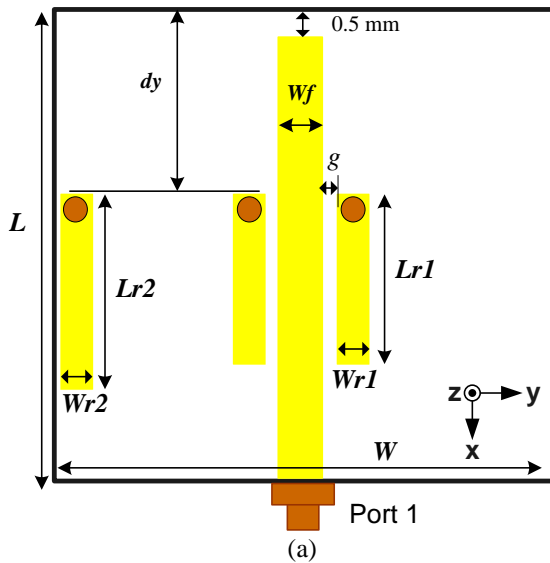
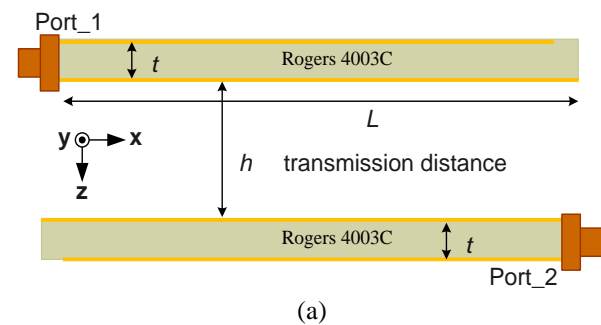


Fig. 1. Top and bottom layers of the proposed design: (a) top layer and (b) bottom layer.

Table 1: List of parameters

Parameter	Value / Type
Substrate	Rogers 4003C
ϵ_r	3.55
Thickness of substrate (t)	0.83 mm
L	20 mm
$Lr1$	8 mm
$Lr2$	11 mm
$Wr1$	1.5 mm
g	0.5 mm
W_f	2 mm
$Wr2$	1.75 mm
W	20 mm
Gr	0.5 mm
$Wr3$	2 mm
$Wr4$	5.5 mm



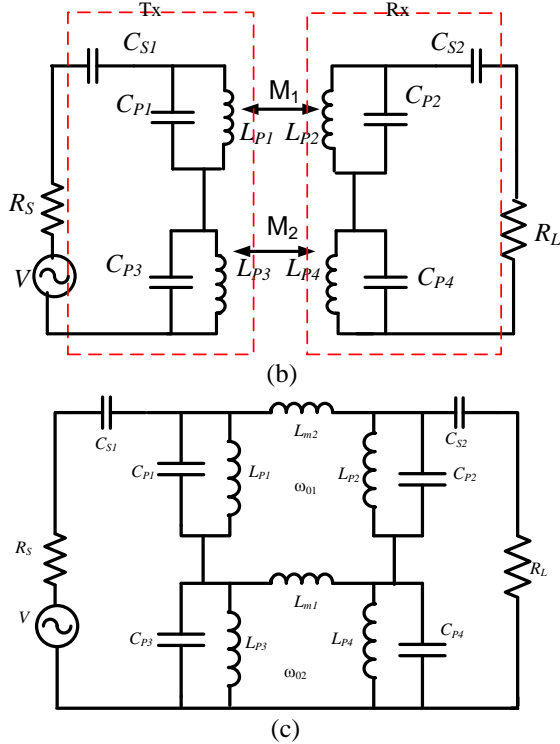


Fig. 2. Equivalent circuit and 3-D view. (a) 3-D view. (b) The equivalent circuit of the system. (c) The pi-equivalent circuit (π) of the system.

It is desired to compute and extract the values of the equivalent circuit parameters (C_p , L_p , L_{m1} , L_{m2} , and C_s) from the simulation consequences for validations. Where M_1 and M_2 are the mutual couplings between two resonators [22], L_{m1} and L_{m2} are the mutual inductances [22], and C_s is the series capacitance. Equations (1) and (2) are employed to calculate the equivalent circuit parameters [21]:

$$C_p = \frac{5f_c}{\pi[f_0^2 - f_c^2]} \text{ pF}, \quad (1)$$

$$L_p = \frac{250}{C_p[\pi f_0]^2} \text{ nH}, \quad (2)$$

where f_c is the cutoff frequency and f_0 is the center resonance frequency at each band alone.

At the first resonance frequency, the frequencies are $f_{c1} = 0.59372$ GHz and $f_{o1} = 0.64793$ GHz. By substitution in equation (1) and (2), the extracted parameters are $C_{p1} = C_{p2} = 14$ pF and $L_{p1} = L_{p2} = 4.29$ nH. In the same way at the second resonance frequency, the frequencies are $f_{c2} = 1.4516$ GHz and $f_{o2} = 1.5613$ GHz. By substitution in equation (1) and (2), the extracted parameters are $C_{p3} = C_{p4} = 6.98$ pF and $L_{p3} = L_{p4} = 1.48$ nH.

Figure 3 compares the simulation results of the equivalent circuit of the proposed design employing the extracted parameters using the advanced design system

(ADS) and the electromagnetic (EM) simulation by the computer simulation technology (CST). The used EM simulator is a 3D full wave solver based on a numerical analysis technique using finite difference time domain (FDTD) approach that computes the S-parameters. As a result, acceptable correspondence is observed between the two results.

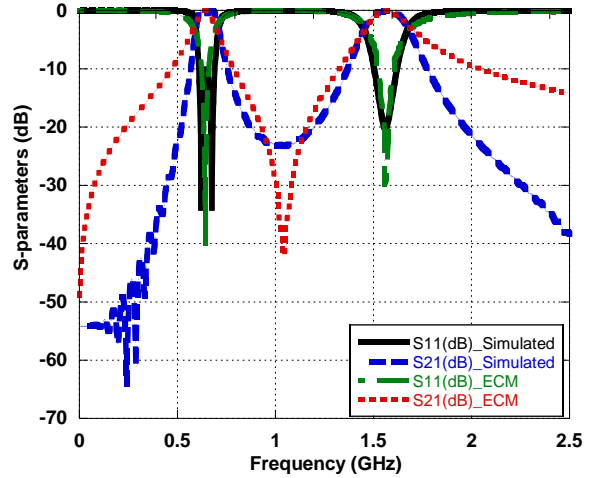
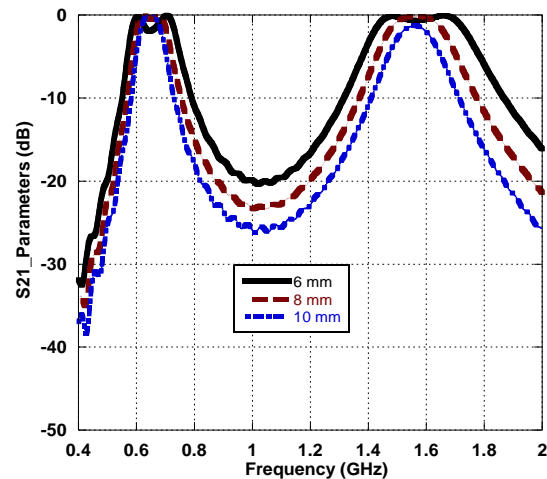


Fig. 3. Comparison between the equivalent circuit (ADS) and EM simulation (CST).

A. The study of transmission distance h

Figure (4) demonstrates the effect of the distance h on the S-parameters. To find out the optimum distance amid Tx (transmitter) and Rx (receiver), the transmission distances are examined within multiple ranges at 6 mm, 8 mm, and 10 mm. The splitting between Tx and Rx is noticeable at 6 mm, while the two resonances are acceptable at 10 mm as discussed in [10]. From this study, the 8 mm separation is a suitable transmission distance to be used for this design.



(a)

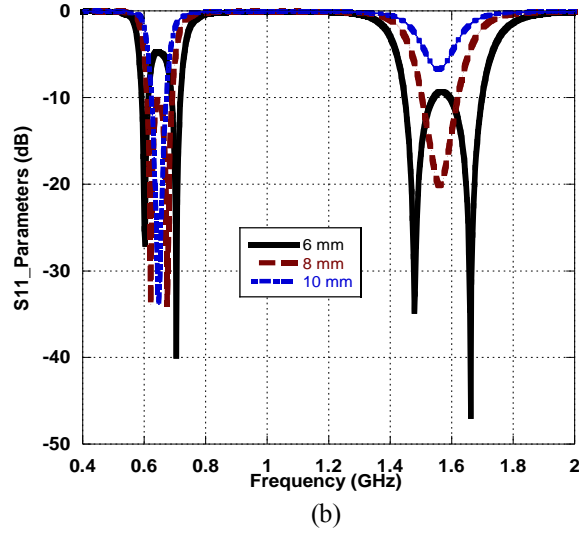


Fig. 4. The study of transmission distance h : (a) S21 parameters and (b) S11 parameters.

B. Parametric study of $Lr2$

Figure 5 shows the effect of changing the length of $Lr2$ from 7 mm to 11 mm. The study displays the changing of the second resonance without any effect on the first resonance frequency. This is suitable for controlling the second resonance while the first resonance is kept constant.

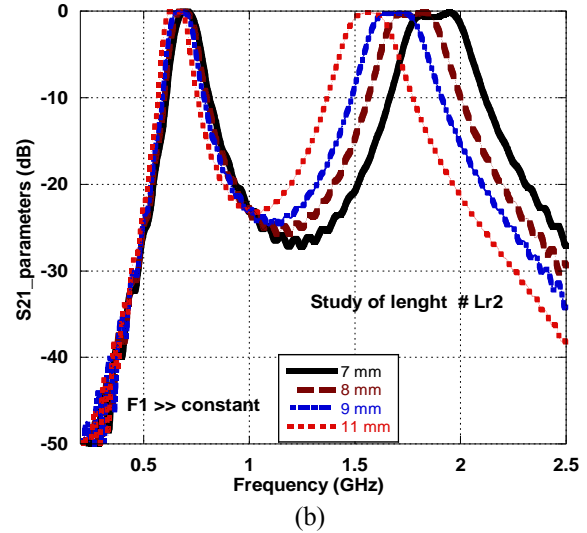
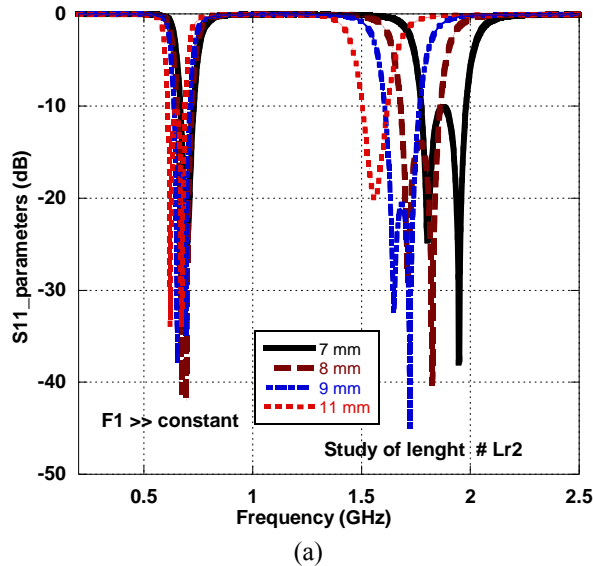


Fig. 5. Parametric study of the length $Lr2$: (a) S11 parameters and (b) S21 parameters.

III. EXPERIMENTAL RESULTS

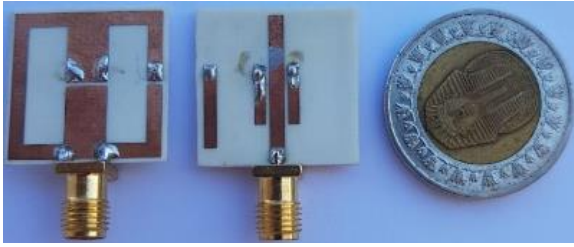
The proposed construction is fabricated and verified for validations with the specifications in Table 1. The fabrication of the proposed structure was done by a photolithographic method and the layers of the fabricated prototype are shown in Fig. 6 (a). Figure 6 (b) shows the configuration of the proposed structure at a separation distance of 8 mm. The measurements are done using the R&S ZVB20 vector network analyzer. The photograph of the fabricated sample is shown in Fig. 6 (a). Figure 6 (c) shows the comparison of the simulation and the measurements. The obtained measurements are in good correspondence with the simulation as displayed in Fig. 6 (c).

The coupling efficiency (η) of the system is calculated using equation (3) [10,20]. The figure of merits (FoM) demonstrates the performance of the system and calculated using equation (4) [10,20]. The measurement results are presented in Fig. 6 (c). The system achieved efficiencies of 72% and 89% at 0.65 GHz and 1.56 GHz at a transmission distance of 8 mm. The estimated FoMs using equation (4) are 0.288 and 0.356 at 0.65 GHz and 1.56 GHz, respectively:

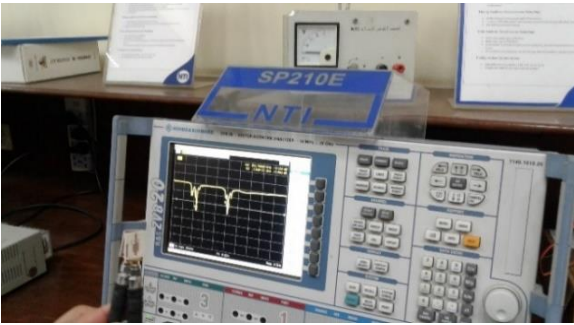
$$\eta = \frac{|s_{21}|^2}{1 - |s_{11}|^2}, \quad (3)$$

$$FoM = \eta \times \frac{h}{\sqrt{A}}, \quad (4)$$

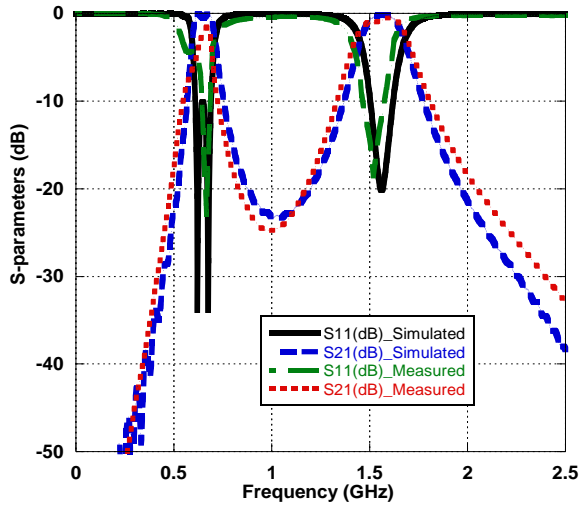
where η is the coupling efficiency and A is the total area of the resonator.



(a)



(b)



(c)

Fig. 6. The fabricated structure and experimental measurements. (a) Top and bottom views. (b) Measurement setting at a distance of 8 mm. (c) comparison between the measurement and simulation at a distance of 8 mm.

Table 2 offers a comparison between the proposed structure and other recent works in terms of size, FoM, efficiency, and separation distance. From Table 2, the proposed design has worthy FoM and size compared to the previous cited works.

Table 2: The differences between the suggested structure and previous works

System	[21]	[17]	[22]	This work
MHz	570 and 2440	0.2 and 6.78	280 and 490	650 and 1560
h (mm)	12	25	6	8
η_{WPT} %	69 and 81	70.6 and 78	91.2 and 79.43	72 and 89
FoM	0.331 and 0.388	0.17 and 0.19	0.27 and 0.23	0.288 and 0.356
Size (mm ²)	25 × 25	125 × 89	20 × 20	20 × 20

IV. CONCLUSION

The dual frequency system is designed, analyzed, and fabricated. The system achieved efficiencies of 72% and 89% at 0.65 GHz and 1.56 GHz, correspondingly at 8 mm separation. The system has a compact size which is suitable for recharging electronics devices and biomedical devices. The experimental performance of the suggested design is in an appropriate concurrence with the simulated one.

REFERENCES

- [1] M. Ghovanloo and K. Najafi, "A modular 32-site wireless neural stimulation microsystem," *IEEE J. Solid-State Circuits*, vol. 39, no. 12, pp. 2457-2466, Dec. 2004.
- [2] S. D. Barman, A. W. Reza, N. Kumar, M. E. Karim, and A. B. Munir, "Wireless powering by magnetic resonant coupling: Recent trends in wireless power transfer system and its applications," *Renew. Sustain. Energy Rev.*, vol. 51, pp. 1525-1552, Nov. 2015.
- [3] M. Kiani and M. Ghovanloo, "An RFID-based closed-loop wireless power transmission system for biomedical applications," *IEEE Trans. Circuits Syst. II Express Briefs*, vol. 57, no. 4, pp. 260-264, Apr. 2010.
- [4] M. Dionigi and M. Mongiardo, "A novel resonator for simultaneous wireless power transfer and near field magnetic communications," *IEEE/MTT-S International Microwave Symposium Digest*, Montreal, QC, Canada, pp. 1-3, June 17-22, 2012.
- [5] S. Barmada and M. Tucci, "Theoretical study of different access points in coupled wireless power transfer – powerline communication systems," *Applied Computational Electromagnetics Society (ACES) Journal*, vol. 33, no. 10, pp. 1112-1116, Oct. 2018.
- [6] M. Ghovanloo and S. Atluri, "A wide-band power-efficient inductive wireless link for implantable microelectronic devices using multiple carriers,"

- IEEE Transactions on Circuits and Systems I: Regular Papers*, vol. 54, no. 10, pp. 2211-2221, Oct. 2007.
- [7] T. Imura, H. Okabe, and Y. Hori, "Basic experimental study on helical antennas of wireless power transfer for electric vehicles by using magnetic resonant couplings," *2009 IEEE Vehicle Power and Propulsion Conference*, Dearborn, MI, USA, pp. 936-940, Sept. 7-10, 2009.
- [8] G. Wang, W. Liu, M. Sivaprakasam, and G. A. Kendir, "Design and analysis of an adaptive transcutaneous power telemetry for biomedical implants," *IEEE Transactions on Circuits and Systems I: Regular Papers*, vol. 52, no. 10, pp. 2109-2117, Oct. 2005.
- [9] D. Kim, A. T. Sutinjo, and A. Abu-Siada, "Near-field analysis and design of inductively-coupled wireless power transfer system in FEKO," *Applied Computational Electromagnetics Society (ACES) Journal*, vol. 35, no. 1, pp. 82-93, Jan. 2020.
- [10] S. Hekal, A. B. Abdel-Rahman, H. Jia, A. Allam, A. Barakat, and R. K. Pokharel, "A novel technique for compact size wireless power transfer applications using defected ground structures," *IEEE Transactions on Microwave Theory and Techniques*, vol. 65, no. 2, pp. 591-599, Feb. 2017.
- [11] F. Tahar, A. Barakat, R. Saad, K. Yoshitomi, and R. K. Pokharel, "Dual-band defected ground structures wireless power transfer system with independent external and inter resonator coupling," *IEEE Transactions on Circuits and Systems II: Express Briefs*, vol. 64, no. 12, pp. 1372-1376, Dec. 2017.
- [12] H. A. Atallah, "Compact and efficient WPT systems using half-ring resonators (HRRs) for powering electronic devices," *Wireless Power Transfer (WPT)*, vol. 5, no. 2, pp. 105-112, Sept. 2018.
- [13] D.-G. Seo, S.-H. Ahn, J.-H. Kim, S.-T. Khang, S.-C. Chae, J.-W. Yu, and W.-S. Lee, "Power transfer efficiency for distance-adaptive wireless power transfer system," *Applied Computational Electromagnetics Society (ACES) Journal*, vol. 33, no. 10, pp. 1171-1174, Oct. 2018.
- [14] R. Sharaf, S. Hekal, A. A. EL-Hameed, A. B. Abdel-Rahman, and R. K. Pokharel, "A new compact wireless power transfer system using C-shaped printed resonators," *2016 IEEE International Conference on Electronics, Circuits and Systems (ICECS)*, Monte Carlo, Monaco, France, pp. 321-323, Dec. 2016.
- [15] R. Hussein, H. A. Atallah, S. Hekal, and A. B. Abdel-Rahman, "A new design for compact size wireless power transfer applications using spiral defected ground structures," *Radioengineering*, vol. 27, no. 4, pp. 1032-1037, Sept. 2018.
- [16] A. Barakat, K. Yoshitomi, and R. K. Pokharel, "Design and implementation of dual-mode inductors for dual-band wireless power transfer systems," *IEEE Transactions on Circuits and Systems II: Express Briefs*, vol. 66, no. 8, pp. 1287-1291, Aug. 2019.
- [17] D. Ahn and P. P. Mercier, "Wireless power transfer with concurrent 200-kHz and 6.78-MHz operation in a single-transmitter device," *IEEE Transactions on Power Electronics*, vol. 31, no. 7, pp. 5018-5029, July 2016.
- [18] H. A. Atallah, R. Hussein, and A. B. Abdel-Rahman, "Novel and compact design of capacitively loaded c-shaped DGS resonators for dual band wireless power transfer (DB-WPT) Systems," *AEU-International Journal of Electronics and Communications*, vol. 100, pp. 95-105, Feb. 2019.
- [19] D. Wang and R. Negra, "Design of a dual-band rectifier for wireless power transmission," *2013 IEEE Wireless Power Transfer (WPT)*, Perugia, Italy, pp. 127-130, May 15-16, 2013.
- [20] S. Verma, D. Rano, and M. Hashmi, "Enhancing the performance of defected ground structure type near-field radiofrequency WPT system by coupled-line impedance matching," *IET Microwaves, Antennas & Propagation*, vol. 14, no. 12, pp. 1431-1439, Oct. 2020.
- [21] M. M. A. El-negm, H. A. Atallah, and A. B. Abdelrahman, "Design of dual-band coupled resonators using complementary split ring resonators defected ground structure (CSRRS-DGS) for wireless power transfer applications," *2020 36th National Radio Science Conference*, Cairo, Egypt, pp. 22-27, June 2019.
- [22] H. A. Atallah, R. Hussein, and A. B. Abdel-Rahman, "Compact coupled resonators for small size dual-frequency wireless power transfer (DF-WPT) systems," *IET Microwaves, Antennas & Propagation*, vol. 14, no. 7, pp. 617-628, May 2020.



Hany A. Atallah was born in Qena, Egypt in 1984. He received his B.Sc. and M.Sc. in Electrical Engineering, Electronics and Communications from South Valley University, Egypt, in 2007 and 2012, respectively. The Ph.D. degree in Antennas and Microwave Engineering at Egypt-Japan University for Science and Technology (E-JUST). He is currently working as an Assistant Professor at the Electrical Engineering Department, Qena Faculty of Engineering, South Valley University. He was a Visiting Researcher with the E-JUST Lab, School of Information

Science and Electrical Engineering, Kyushu University, Japan, from September 2015 to July 2016. His research interests include antenna design, dielectric resonators, metamaterials, tunable filters, reconfigurable antennas, antenna arrays, microwave filters, and FDTD. His recent research has been on cognitive radio (CR) antennas, wireless power transfer (WPT) for biomedical implants, electric vehicles, and electronic devices, breast cancer detection, smart meters, and the internet of things (IoT).



Musallam Alzubi was born in Kuwait. He received his B.Sc. in Electrical Engineering, Electronics and communication from Al-Ahliyya Amman University, Jordan, in 2016. He is currently working toward his M.Sc. at the Electrical Engineering Department, Qena Faculty of Engineering, South Valley University. He is currently working at Ministry of Communications at Kuwait. His research interests include filter design, and wireless power transfer (WPT) for biomedical implants and electronic devices.

Rasha Hussein was born in Qena, Egypt. She received her B.Sc. in Electrical Engineering, Electronics and communication from South Valley University, Egypt, in 2015. She is currently working as a Teaching Assistant at the Electrical Engineering Department, Qena Faculty of Engineering, South Valley University. Her research interests include antenna design, filter design, and wireless power transfer (WPT) for biomedical implants and electronic devices.



Adel B. AbdelRhman was born in Aswan, Egypt, in 1968. He received the B.Sc. and M.Sc. degrees in Electrical Engineering, Communication and Electronics, Assuit University, Egypt, in 1991 and 1998, respectively. The Ph.D. degree in Microwave Engineering at the University of Magdeburg, Magdeburg, Germany. He is currently working as Assoc. Prof. at the E-JUST, Alexandria, Egypt-on leave from the South Valley University, Qena 83523, Egypt. His research interests include the design and analysis of microstrip antennas, filters, and its application in WLAN and mobile communication. His recent research has been on cognitive radios, wireless power transfer, and on-chip antennas.